Precise and Accurate Measurements of Strong-Field Photoionization and a Transferable Laser Intensity Calibration Standard

W. C. Wallace, O. Ghafur, C. Khurmi, Satya Sainadh U, J. E. Calvert, D. E. Laban, M. G. Pullen, K. Bartschat, A. N. Grum-Grzhimailo, D. Wells, H. M. Quiney, X. M. Tong, I. V. Litvinyuk, R. T. Sang, and D. Kielpinski

Phys. Rev. Lett. **117**, 053001 — Published 29 July 2016

DOI: 10.1103/PhysRevLett.117.053001

Precise and accurate measurements of strong-field photoionisation and a transferrable laser intensity calibration standard

W.C. Wallace,[1,2] O. Ghafur,[1,2] C. Khurmi,[1,2] Satya Sainadh U,[1,2] J.E. Calvert,[1,2] D.E. Laban,[1,2] M.G. Pullen,[1,2,*] K. Bartschat,[1,2,3] A.N. Grum-Grzhimailo,[4] D. Wells,[5] H.M. Quiney,[5] X.M. Tong,[6] I.V. Litvinyuk,[2] R.T. Sang,[1,2] and D. Kielpinski[1,2,†]

[1] *ARC Centre of Excellence for Coherent X-Ray Science, Griffith University, Brisbane, Queensland, Australia*
[2] *Australian Attosecond Science Facility and Centre for Quantum Dynamics, Griffith University, Brisbane, Queensland, Australia*
[3] *Department of Physics and Astronomy, Drake University, Des Moines, Iowa 50311, USA*
[4] *Skobeltsyn Institute of Nuclear Physics, Lomonosov Moscow State University, Moscow 119991, Russia*
[5] *ARC Centre of Excellence for Coherent X-Ray Science, University of Melbourne, Melbourne, Victoria, Australia*
[6] *Division of Materials Science, Faculty of Pure and Applied Sciences, and Center for Computational Science, University of Tsukuba, 1-1-1 Tennodai, Tsukuba, Ibaraki 305-8577, Japan*

Ionization of atoms and molecules in strong laser fields is a fundamental process in many fields of research, especially in the emerging field of attosecond science. So far, demonstrably accurate data have only been acquired for atomic hydrogen (H), a species that is accessible to few investigators. Here we present measurements of the ionization yield for argon, krypton, and xenon with percent-level accuracy, calibrated using H, in a laser regime widely used in attosecond science. We derive a transferrable calibration standard for laser peak intensity, accurate to 1.3%, that is based on a simple reference curve. In addition, our measurements provide a much-needed benchmark for testing models of ionisation in noble-gas atoms, such as the widely employed single-active electron approximation.

Ionization by strong laser fields drives processes ranging from attosecond pulse generation [1, 2] to filamentation [3] and remote lasing [4]. Measurements of strong-field ionization have revealed complex and surprising qualitative features [5, 6] that can depend sensitively on the laser intensity. Precise measurements of strong-field ionization are now being used to probe fundamental physics, such as time delays in photoionization [7], but there is substantial evidence that small systematic offsets in these measurements can obscure the results [8]. In frequency metrology, measurements of atomic transitions are affected by systematic errors arising from the AC-Stark shift and laser intensity uncertainty, thereby limiting the precision of the result [9]. Accurate reference data on strong-field photoionization and laser intensity, especially in the attosecond science regime, are therefore needed for further progress on these questions.

In recent years, our group has used atomic hydrogen (H) to perform quantitatively accurate strong-field measurements that are demonstrably free from systematic errors [10–12]. These measurements are performed in the regime of laser pulse durations and peak intensities that are most widely used in attosecond science. As the simplest electronic system, H has long been recognised as a benchmark species for strong-field physics experiments [13, 14]. Direct integration of the three-dimensional time-dependent Schrödinger equation (3D-TDSE) enables high-accuracy simulation of H and less than 1% error, with only very minor approximations [15]. Hence, the accuracy of the H data can be certified by their agreement with 3D-TDSE simulations.

Here we use these techniques to perform accurate measurements of the strong-field ionization yield from three commonly used noble-gas targets, and to derive a transferrable, high-accuracy calibration standard for laser intensity. Our data enable accurate inter-comparisons of data taken at various strong-field laboratories; and improved simulations of complex phenomena involving strong-field ionisation, such as filamentation, high-harmonic generation, and laser-induced electron diffraction. We use the noble-gas data to derive a calibration standard for laser peak intensity, given by a simple reference curve, that offers an order of magnitude better accuracy than previous transferrable standards [16, 17]. Our intensity calibration standard applies to an intensity regime that is readily transferrable to laboratories using few-cycle 800 nm laser systems, including most attosecond science laboratories.

The experimental apparatus is detailed in [10, 11]. It consists of a well-collimated atomic H beam skimmed from the output of an RF discharge dissociator, which intersects the focus of an intense few-cycle laser. The flux of our custom-constructed atomic source is several orders of magnitude higher than commercial sources [18], facilitating a high signal level. The laser generates pulses with rapidly varying carrier-envelope phase (CEP) of 5.5 fs duration (measured at full-width at half-maximum of intensity) with a central wavelength of 800 nm. Pre- and

post-pulse effects were observed to be minimal due to the absence of sidelobes in the autocorrelation trace. Ions are created in the overlap region between the atomic beam and the laser beam, and are detected with an ion time-of-flight (ion-TOF) mass spectrometer. A microchannel plate (MCP) located at the end of the ion-TOF detects the ions and outputs a voltage proportional to the ion yield (see Supplementary Information). The overlap region is well-defined, allowing us to account accurately for focal-volume averaging (FVA) effects [12].

The measured yield of H^+ ions resulting from ionisation of atomic H over a range of laser peak intensities is shown in Fig. 1. This yield, denoted Y_{H^+}, is accurately measured by removing contributions arising from ionisation of undissociated H_2 in the beam, and background H_2O vapour. These contaminant signals can be as large as 9.5% of the desired Y_{H^+}, and hence must be removed to obtain percent-level accuracy. Errors in Y_{H^+} accumulate from MCP voltage baseline subtraction, from short- and long-term laser drifts, and from uncertainties in determining the dissociation fraction. A detailed account of the analysis and error estimation is given in the Supplementary Information.

We certify the accuracy of our data by comparison with accurate 3D-TDSE calculations. As in our previous work [10, 11], we perform FVA over the interaction volume, assuming a Gaussian laser profile and a molecular beam of diameter d, where d is much smaller than the laser Rayleigh range and much larger than the transverse size of the laser beam. Under these conditions, the FVA becomes independent of beam propagation effects [12]. Effects of CEP on the theoretical yields were negligible. We perform a weighted least-squares fit of the 3D-TDSE yield predictions to the Y_{H^+} data using a function of the form

$$P_{H^+}(I_{est}, A, \eta_1) = A \cdot S(\eta_1 I_{est}). \quad (1)$$

Here A and η_1 are the fit parameters, while S is the focal-volume averaged and carrier-envelope-phase averaged theory model evaluated at the actual laser intensity $I_0 = \eta_1 I_{est}$. The independently estimated intensity I_{est} is obtained from measurements of the laser parameters – waist size w_0, average power P, pulse duration τ_p, and repetition rate f_{rep} – via

$$I_{est} = \frac{2P}{\pi w_0^2} \frac{1}{f_{rep}\tau_p}. \quad (2)$$

The η_1 fit parameter is a rescaling coefficient of the laser intensity that accounts for the error in I_{est}(often as large as 50%), and permits the accurate retrieval of I_0. The A fit parameter rescales the yield to account for both the unknown atomic density and detector efficiency, but is irrelevant for intensity calibration.

Figure 1 illustrates the agreement between the Y_{H^+} data and the 3D-TDSE simulations, certifying that

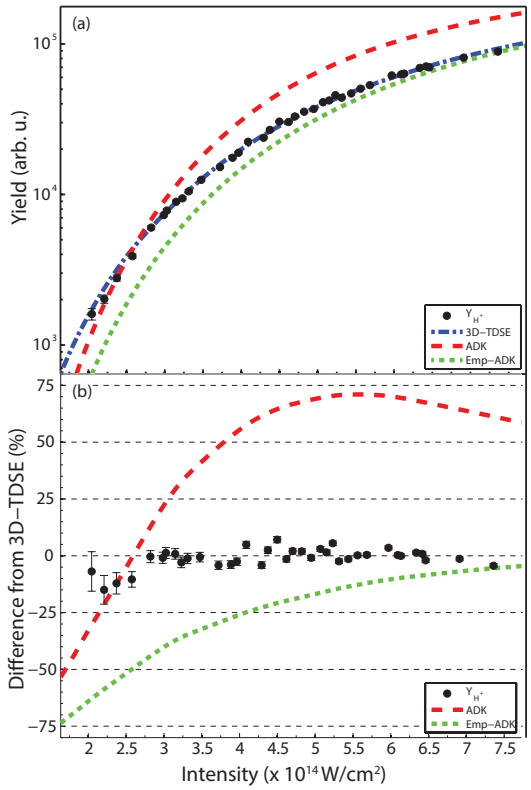

FIG. 1. (a) Experimental data for H^+ yield (solid circles), compared with theoretical predictions from 3D-TDSE (dot-dashed line), standard ADK (dashed line), and empirically corrected ADK (Emp-ADK; dotted line) models. In some cases, the error bars on the data are smaller than the symbols; see Supplementary Information for error estimates. (b) Percentage difference of experimental H^+ yield data and both ADK theories from the 3D-TDSE simulations.

our data are free of systematic error to within our 2% measurement precision. A value of $\eta_1 = 0.641 \pm 0.007$ is found, indicating that we can calibrate the laser peak intensity to a theory-certified accuracy of better than 1.1% without systematic error. Normalized residuals from the fit are shown as percentage deviations from the 3D-TDSE predictions in Fig. 1. Neglecting background subtraction shifts η_1 by 3.1%, more than our 1.1% accuracy.

Our data are easily able to discriminate between the 3D-TDSE and other commonly used theoretical approximations. A well-known alternative to solving the TDSE is the analytic theory of Ammosov, Delone and Krainov (ADK) [19]. Standard ADK theory is intuitive and straightforward to calculate, but it is known to fail at intensities near to or exceeding the onset of barrier-suppressed ionization (BSI) [20]. An empirical correction [21] has since been developed to extend the validity of ADK rates to higher intensities. Standard ADK and empirically corrected ADK rates, as well as percentage residuals have also been plotted in Fig. 1 using the A and η_1 fit parameters obtained from the 5.5 fs 3D-TDSE fit. Standard ADK deviates from the data at high in-

tensities by almost a factor of two, whereas empirically corrected ADK is accurate at the 10% level there. Nevertheless, the latter model is still clearly ruled out by the data at lower intensities.

We now present demonstrably accurate measurements of the photoionization yield of singly-charged argon, krypton and xenon, providing reference data in a regime for which accurate simulations are not available. Depletion of the noble gas atoms to multiply-charged states was observed but the effect found to be negligible in this intensity regime. The results for the yield of each gas target, denoted Y_{Ar^+}, Y_{Kr^+}, and $Y_{Xe^+}$are shown in Fig. 2. The agreement between theory and experiment for H certifies the accuracy of the noble-gas yields, as these measurements were performed in the same apparatus, using identical laser parameters.

Theoretical ionisation probabilities for the noble-gas atoms are obtained by solving the 3D-TDSE under the single-active electron approximation with the second-order-split operator method in the energy representation [22, 23]. The model potentials [21] are calculated by using the density functional theory with self-interaction correction [24], from which the calculated atomic ionisation potentials are in good agreement with the measured ones. The theoretical simulations are subjected to FVA for comparison with experimental data. As with the atomic H data, we also compare standard ADK and empirically corrected ADK rates with the noble-gas data, using a weighted sum of $m_\ell = 0$, 1 for the p-orbital ($\ell = 0$) and ground-state ionisation potentials. As a non-relativistic model was used, the fine-structure splitting was ignored. We note the existence of fast dynamics due to spin-orbit coupling as investigated in [25], however analysis of these dynamics is outside the scope of this manuscript.

Each of the theory models is compared to Y_{NG^+}(where the subscript NG denotes one of the noble gases) using the calibrated intensity I_0 and the fitting method Eq. (1). The fits and residuals for each target are shown in Fig. 2. Since the intensity is already calibrated by the Y_{H^+} data, the calibration factor η_1 is fixed to a value of 1, whilst A is allowed to vary in order to account for the unknown gas density. While the data are accurate at the 2% level, the theoretical predictions agree with the data only at the tens of percent level, with both ADK rates performing poorly. These data therefore pose a direct challenge to current models which are widely used to predict results from strong-field ionization experiments. Due to the constrained fit parameter, ADK and Emp-ADK fits are weighted more heavily towards the higher intensities because the signal-to-noise is higher and the uncertainty is correspondingly lower. This results in an artefact where ADK appears to fit better than Emp-ADK. Removing the constraint on the η parameter vastly improves the fit, however the retrieved η is significantly different in comparison to the phenomenological model.

TABLE I. Fit parameters used in Eq. (4) for the Ar^+, Kr^+, and Xe^+ gas targets.

Fit Parameter	Ar^+	Kr^+	Xe^+
α (arb. units)	2.84	4.24	3.71
γ (arb. units)	-3.03	-2.49	-2.69
I_c ($\times 10^{14}$ W/cm^2)	3.86 ± 0.05	2.06 ± 0.03	1.18 ± 0.03

While all three theories disagree with the experimental data, Fig. 2 shows that we can achieve good agreement with the data using the following phenomenological model

$$P^{(2D)}_{NG^+}(I_{est}; A, \eta_2) = A \cdot S_{phenom}(\eta_2 I_{est}), \qquad (3)$$

where

$$S_{phenom}(\eta_2 I_{est}) = \frac{\exp\Big(-\alpha\big(\eta_2 I_{est}/I_c\big)^{-1/2}\Big)}{1+\big(\eta_2 I_{est}/I_c\big)^{\gamma}}. \qquad (4)$$

Here A and η_2 are the same fit parameters as described in Eq. (1). The coefficients α and γ are set by fitting Eq. (4) to the 3D-TDSE for each gas target. The value of I_c was determined from the data of Fig. 2 by fixing η_2 to a value of 1, and substituting I_{est} with our I_0 values obtained from the H^+ fit. The values of these parameters are shown in Table I for each gas target. Our values for I_c include the uncertainty in the H^+ calibration as well as the fit error, and demonstrate our ability to calibrate the intensity at the 1.3%, 1.5%, and 2.5% levels using Ar, Kr, and Xe as gas targets respectively[1]. The value of I_c is insensitive against the removal of any individual data point from the fit dataset, indicating that the model robustly represents the data over the entire intensity range. However, it is important to note that the phenomenological model is introduced purely as a convenience, so that the reader can easily carry out intensity calibration with a closed-form analytic fit function. We emphasize that Eq. (4) is not associated with any model of the ionization physics. Hence, we do not expect it to be valid outside the range of intensities studied here.

Equation (4) enables absolute intensity calibration at the 1.3% level for few-cycle 800 nm laser systems, like those widely used for attosecond science. The calibration only requires a mass spectrometer, a few-cycle laser at 800 nm, and a source of either Ar, Kr, or Xe. The intensity range covered by our calibration, $1 - 5 \times 10^{14}$ W/cm^2, is used by most atomic and molecular strong-field physics experiments, particularly attosecond science experiments. Instructions for using our calibration are detailed in the Supplementary Information.

Our transferrable calibration standard can be shown to reliably determine the *absolute* intensity without systematic errors; in other words, the retrieved intensity

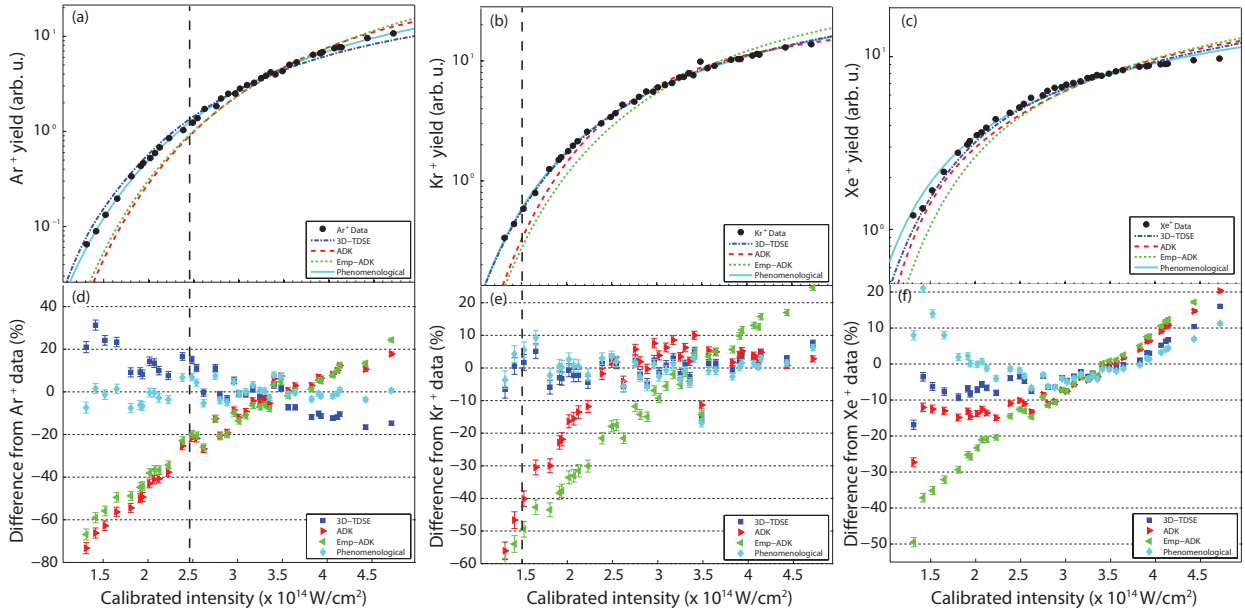

FIG. 2. (Color online) Top row: intensity-calibrated experimental data (black circles) for (a) Ar^+, (b) Kr^+, and (c) Xe^+ compared with theoretical predictions from 3D-TDSE (blue, dot-dashed line), ADK (red, dashed line), and Emp-ADK (green, dotted line) models, as well as the phenomenological model given by Eq. (3) (cyan, solid line). The only fit parameter is the overall rescaling of yield, A. In some cases, the error bars on the data are smaller than the symbols. Bottom row: normalized residuals for (d) Ar^+, (e) Kr^+, and (f) Xe^+, for each theoretical prediction, shown as percentage deviations from the experimental yield data for the respective gas targets. Dashed black line indicates barrier-suppression threshold (Xe threshold off-scale at 9×10^{13} W/cm^2).

can be accurately expressed in the SI unit of W/m^2. Previously presented transferrable intensity calibration methods [17, 26, 27] relied on theoretical approximations whose systematic errors were not fully quantified. The removal of systematic errors, i.e., offsets between the measured value and the "true value" of the measured quantity [28], is crucial for accurate measurement. Therefore, while these previous methods provide *relative* calibrations of the intensities in the interaction region, their relationship to the SI system of units remains unclear.

Our calibration is relatively insensitive to laser parameters other than peak intensity. As shown in our previous work [11], variations of the pulse duration by 10% may cause a rescaling of the overall yield, but cause $< 1\%$ shifts in the retrieved intensity. Similarly, the calibration is not overly sensitive to the precise form of the beam profile: we achieve good theory-experiment agreement for H with beam M^2 factors as high as 1.5. In most experiments with molecular beams, including ours, the focal volume averaging is independent of M^2 so long as the transverse intensity distribution is Gaussian and is constant within the interaction region. As long as these conditions are satisfied, Eq. (4) is expected to hold even for much larger values of M^2. While the calibration can presently only be used for wavelengths near 800 nm, our simulations show that changes of the wavelength by 50 nm affect the retrieved intensity by $< 1\%$. This lack of sensitivity is expected since our laser bandwidth is > 200 nm. Finally, the calibration can tolerate laser pulse energy fluctuations of at least 0.7% (root-mean-square), as independently measured on a photodiode. We achieve good theory-experiment agreement for H at this level.

Other laboratories can transfer our calibration standard to lasers of widely different pulse durations or wavelengths, without the use of an H source, by the following procedure. (i) Calibrate the intensity of a standard few-cycle laser near 800 nm by measuring one of Ar^+, Kr^+, or Xe^+ photoion yields. (ii) Measure the ratios of the beam parameters used in Eq. (2) between the new and standard laser. These ratios can be measured much more accurately than the parameters themselves. From these ratios, derive an absolute calibration of the new laser's intensity. (iii) Measure Ar^+, Kr^+, or Xe^+ photoion yield as a function of the new laser's intensity. The data for the new laser are known to be accurate, since they are referenced to our data by steps (i) and (ii). Finally, (iv) construct a phenomenological fitting function for the new data, to be used in the same way as Eq. (3) above. A method for intensity calibration for apparatus, in which an atomic beam is not employed, has also been provided in the Supplementary Information.

We have presented photoionization yield measurements with an accuracy that improves on previous measurements by an order of magnitude. Our data are obtained in a regime of laser pulse duration and intensity that is widely used for attosecond science, and can

be used to benchmark measurement techniques in that field. The measurements are certified at the percent level through the observation of theory-experiment agreement for H. Using the noble-gas data presented here, other laboratories can verify the accuracy of their measurements, calibrate their apparatus, and obtain similarly accurate data for other atomic and molecular species. In the meantime, our data provide accurate reference for simulations of strong-field phenomena involving few-cycle ionization. Finally, we have presented a transferrable calibration of laser intensity that provides an order-of-magnitude accuracy improvement. The standard is readily accessible to laboratories using few-cycle 800 nm lasers and can be further transferred to other laser systems, enabling the correct measurement and interpretation of intensity-sensitive phenomena in strong-field ionization.

This work was supported by the United States Air Force Office of Scientific Research under Grant FA2386-12-1-4025 and by the Australian Research Council (ARC) Centre of Excellence for Coherent X-Ray Science under Grant CE0561787. W.C.W., J.E.C., M.G.P., and D.E.L. were supported by Australian Postgraduate Awards. K.B. acknowledges support from the United States National Science Foundation under Grant No. PHY-1430245 and the XSEDE Allocation No. PHY-090031. X.M.T. was supported by a Grant-in-Aid for Scientific Research (No. C24540421) from the Japan Society for the Promotion of Science. Some calculations were carried out by the supercomputer of the HA-PACS project for advanced interdisciplinary computational sciences by exa-scale computing technology, others on Stampede at the Texas Advanced Computer Center. D.K. was supported by ARC Future Fellowship FT110100513.

* Now at: ICFO-Institut de Ciències Fotòniques, Av. Carl Friedrich Gauss 3, 08860 Castelldefels (Barcelona), Spain
† Corresponding author: d.kielpinski@griffith.edu.au

[1] P. B. Corkum and F. Krausz, Nature Phys. **3**, 381 (2007).
[2] T. Popmintchev, M.-C. Chen, P. Arpin, M. M. Murnane, and H. C. Kapteyn, Nature Photon. **4**, 822 (2010).
[3] L. Bergé, S. Skupin, R. Nuter, J. Kasparian, and J.-P. Wolf, Rep. Prog. Phys. **70**, 1633 (2007).
[4] P. R. Hemmer, R. B. Miles, P. Polynkin, T. Siebert, A. V. Sokolov, P. Sprangle, and M. O. Scully, Proc. Natl. Acad. Sci. USA **108**, 3130 (2011).
[5] F. Grasbon, G. Paulus, H. Walther, P. Villoresi, G. Sansone, S. Stagira, M. Nisoli, and S. De Silvestri, Phys. Rev. Lett. **91**, 173003 (2003).
[6] J. Wassaf, V. Véniard, R. Taïeb, and A. Maquet, Phys. Rev. Lett. **90**, 013003 (2003).
[7] P. Eckle, A. Pfeiffer, C. Cirelli, A. Staudte, R. Dörner, H. Muller, M. Büttiker, and U. Keller, Science **322**, 1525 (2008).
[8] L. Torlina, F. Morales, J. Kaushal, H. G. Muller, I. Ivanov, A. Kheifets, A. Zielinski, A. Scrinzi, M. Ivanov, and O. Smirnova, arXiv:1402.5620 (2014).
[9] A. Marian, M. C. Stowe, J. R. Lawall, D. Felinto, and J. Ye, Science **306**, 2063 (2004).
[10] M. G. Pullen, W. C. Wallace, D. E. Laban, A. J. Palmer, G. F. Hanne, A. N. Grum-Grzhimailo, B. Abeln, K. Bartschat, D. Weflen, I. Ivanov, A. Kheifets, H. M. Quiney, I. V. Litvinyuk, R. T. Sang, and D. Kielpinski, Opt. Lett. **36**, 3660 (2011).
[11] M. Pullen, W. Wallace, D. Laban, A. Palmer, G. Hanne, A. Grum-Grzhimailo, K. Bartschat, I. Ivanov, A. Kheifets, D. Wells, H. Quiney, X. Tong, I. Litvinyuk, R. Sang, and D. Kielpinski, Phys. Rev. A **87**, 053411 (2013).
[12] D. Kielpinski, R. T. Sang, and I. V. Litvinyuk, J. Phys. B **47**, 204003 (2014).
[13] H. Rottke, D. Feldmann, B. Wolff-Rottke, and K. H. Welge, J. Phys. B **26**, L15 (1993).
[14] G. G. Paulus, W. Nicklich, F. Zacher, P. Lambropoulos, and H. Walther, J. Phys. B **29**, L249 (1996).
[15] A. N. Grum-Grzhimailo, B. Abeln, K. Bartschat, D. Weflen, and T. Urness, Phys. Rev. A **81**, 043408 (2010).
[16] C. Smeenk, J. Z. Salvail, L. Arissian, P. B. Corkum, C. T. Hebeisen, and A. Staudte, Opt. Express **19**, 9336 (2011).
[17] S. Micheau, Z. Chen, A. T. Le, J. Rauschenberger, M. F. Kling, and C. D. Lin, Phys. Rev. Lett. **102**, 073001 (2009).
[18] M. G. Pullen, *Above threshold ionisation of atomic hydrogen using few-cycle pulses*, Ph.D. thesis, Griffith University, Brisbane, Australia (2011), available at http://libraryguides.griffith.edu.au/theses.
[19] M. V. Ammosov, N. B. Delone, and V. P. Krainov, Sov. Phys. JETP **64**, 1191 (1986).
[20] C. Spielmann, C. Kan, N. H. Burnett, T. Brabec, M. Geissler, A. Scrinzi, M. Schnurer, and F. Krausz, IEEE J. Sel. Top. Quant. Elec. **4**, 249 (1998).
[21] X. Tong and C. Lin, Journal of Physics B: Atomic, Molecular and Optical Physics **38**, 2593 (2005).
[22] X. M. Tong, K. Hino, and N. Toshima, Phys. Rev. A **74**, 031405 (2006).
[23] X.-M. Tong and S.-I. Chu, Chemical Physics **217**, 119 (1997), dynamics of Driven Quantum Systems.
[24] X.-M. Tong and S.-I. Chu, Phys. Rev. A **55**, 3406 (1997).
[25] N. Rohringer and R. Santra, Physical Review A **79**, 053402 (2009).
[26] S. Larochelle, A. Talebpour, and S. Chin, J. Phys. B **31**, 1215 (1998).
[27] I. V. Litvinyuk, K. F. Lee, P. W. Dooley, D. M. Rayner, D. M. Villeneuve, and P. B. Corkum, Phys. Rev. Lett. **90**, 233003 (2003).
[28] Joint Committee for Guides in Metrology, *JCGM 100:2008. Evaluation of measurement data – Guide to the expression of uncertainty in measurement*, Geneva, Switzerland (2008).

[1] Per the recommendations of the Joint Committee for Guides in Metrology [28], we have here stated the 1σ standard deviation for I_c, i.e., the 68% confidence interval. Therefore, on any particular reproduction of our experiment, the retrieved intensity has a 32% probability of falling outside the 68% confidence interval for purely statistical reasons.